Developmental Cell
Article

Noncanonical Wnt Signaling through G Protein-Linked PKCδ Activation Promotes Bone Formation

Xiaolin Tu,[1] Kyu Sang Joeng,[1,2] Keiichi I. Nakayama,[4] Keiko Nakayama,[5] Jayaraj Rajagopal,[6] Thomas J. Carroll,[6,7] Andrew P. McMahon,[6] and Fanxin Long[1,2,3,*]
[1] Department of Medicine
[2] Division of Biology and Biomedical Sciences
[3] Department of Molecular Biology and Pharmacology
Washington University Medical School, St. Louis, MO 63110, USA
[4] Department of Molecular and Cellular Biology, Kyushu University, Fukuoka, Japan
[5] Center for Translational and Advanced Animal Research on Human Diseases, Tohoku University Graduate School of Medicine, Sendai, Japan
[6] Department of Molecular and Cellular Biology, Harvard University, Cambridge, MA 02138, USA
[7] Department of Internal Medicine, Department of Molecular Biology, University of Texas Southwestern Medical Center, Dallas, TX 75390, USA
*Correspondence: flong@wustl.edu
DOI 10.1016/j.devcel.2006.11.003

SUMMARY

Wnt signaling regulates a variety of developmental processes in animals. Although the β-catenin-dependent (canonical) pathway is known to control cell fate, a similar role for noncanonical Wnt signaling has not been established in mammals. Moreover, the intracellular cascades for noncanonical Wnt signaling remain to be elucidated. Here, we delineate a pathway in which Wnt3a signals through the $G\alpha_{q/11}$ subunits of G proteins to activate phosphatidylinositol signaling and PKCδ in the murine ST2 cells. $G\alpha_{q/11}$-PKCδ signaling is required for Wnt3a-induced osteoblastogenesis in these cells, and *PKCδ* homozygous mutant mice exhibit a deficit in embryonic bone formation. Furthermore, Wnt7b, expressed by osteogenic cells in vivo, induces osteoblast differentiation in vitro via the PKCδ-mediated pathway; ablation of *Wnt7b* in skeletal progenitors results in less bone in the mouse embryo. Together, these results reveal a Wnt-dependent osteogenic mechanism, and they provide a potential target pathway for designing therapeutics to promote bone formation.

INTRODUCTION

The Wnt family of proteins are conserved from coelenterate to human and regulate cell proliferation, fate specification, polarity, and migration (Cadigan and Nusse, 1997; Lee et al., 2006). In the canonical Wnt pathway (Huelsken and Birchmeier, 2001; Wodarz and Nusse, 1998), Wnt binding to Frizzled receptors and the low-density lipoprotein receptor-related protein 5 or 6 (LRP5/6) in vertebrates (Mao et al., 2001b; Pinson et al., 2000; Tamai et al., 2000) stabilizes β-catenin and thereby activates transcription of downstream target genes via lymphoid enhancer binding factor-1 (Lef-1) and T cell factors (Tcf1, 3, 4). The amplitude of signaling is fine tuned in part via negative feedback mechanisms that include the secreted molecule Dickkopf 1 (Dkk1) (Glinka et al., 1998), itself a direct transcriptional target of canonical Wnt signaling (Chamorro et al., 2005; Niida et al., 2004). Dkk1 antagonizes the pathway by interfering with LRP5/6 and Wnt interactions (Bafico et al., 2001; Mao et al., 2001a; Semenov et al., 2001).

Wnts also signal through β-catenin-independent (noncanonical) mechanisms to regulate morphogenesis during vertebrate development (Veeman et al., 2003). Most notably, noncanonical Wnt signaling has been implicated in convergence and extension of the body axis during embryogenesis in *Xenopus* (Tada and Smith, 2000; Wallingford et al., 2000), zebrafish (Heisenberg et al., 2000), and mice (Kibar et al., 2001; Wang et al., 2006). In addition, noncanonical Wnt signaling was shown to regulate both polarized extension and planar cell polarity (PCP) in the mouse cochlea (Curtin et al., 2003; Kibar et al., 2001; Montcouquiol et al., 2003; Wang et al., 2005). Thus, noncanonical Wnt signaling directs cell polarity and cell movement in a variety of vertebrate species.

The intracellular cascade responsible for noncanonical Wnt signaling in vertebrates is not well understood. Overexpression of *Xenopus* Wnt5a, rat Frizzled 2, or a *Xenopus* Dishevelled (Dvl) construct lacking the DIX domain (XDshΔDIX) in *Xenopus* or zebrafish embryos stimulated calcium flux and PKC activity by activating phosphatidylinositol signaling sensitive to pertussis toxin (Kuhl et al., 2000; Sheldahl et al., 2003; Slusarski et al., 1997). However, the role of classic PKC is not known, although PKCδ, a novel PKC isoform, was shown to regulate

Xenopus convergent extension in response to Frizzled signaling (Kinoshita et al., 2003). Neither is it known whether a similar signaling cascade operates in mammalian cells. In addition, certain Wnts or Frizzled molecules were found to activate the Rho family of small GTPases in HEK293T cells and *Xenopus* embryos (Habas et al., 2003; Habas et al., 2001). The pathway was implicated in convergent extension in *Xenopus* embryos (Choi and Han, 2002; Habas et al., 2001, 2003; Penzo-Mendez et al., 2003), but a similar role has not been demonstrated in mammals.

The importance of canonical Wnt signaling in bone is supported by genetic evidence from mammals. In humans, loss- or gain-of-function mutations in LRP5 were linked with the osteoporosis-pseudoglioma syndrome (Gong et al., 2001) and a high-bone-density syndrome (Boyden et al., 2002; Little et al., 2002), respectively. Mice lacking LRP5 (*LRP5*$^{-/-}$) (Kato et al., 2002) or Wnt10b (*Wnt10b*$^{-/-}$) (Bennett et al., 2005) exhibited a postnatal low-bone-mass phenotype. Conversely, mice lacking the Wnt antagonist secreted Frizzled-related protein 1 (*sFRP1*$^{-/-}$) developed more bone postnatally (Bodine et al., 2004). Moreover, genetic deletion of β-catenin from early osteoprogenitors resulted in a lack of mature osteoblasts in the mouse embryo (Day et al., 2005; Hill et al., 2005; Hu et al., 2005; Rodda and McMahon, 2006), whereas forced activation of β-catenin greatly enhanced osteogenesis (Rodda and McMahon, 2006). Specifically, β-catenin was shown to be required both prior to *Osterix* (*Osx*) expression (Hu et al., 2005) and for the progression of *Osx*-positive cells to mature osteoblasts (Rodda and McMahon, 2006). Finally, β-catenin signaling in more mature osteoblasts was found to indirectly control bone mass by regulating osteoclast formation through the control of *Osteoprotegerin* expression (Glass et al., 2005).

A role for noncanonical Wnt signaling in bone has not been described. Here, we report a Wnt-G$\alpha_{q/11}$-PKCδ noncanonical pathway that operates in mammalian osteoprogenitors to promote osteoblast development. We further demonstrate that Wnt7b likely promotes bone formation in the mouse in part via this mechanism.

RESULTS

Wnt3a Induces Osteoblastogenesis Coupled with PKC Activation in ST2 Cells

To investigate the molecular mechanism underlying Wnt signaling during osteoblast differentiation, we established a Wnt-responsive osteoblastogenesis system. The murine bone marrow-derived stromal cell line ST2 (Ogawa et al., 1988), upon incubation with a conditioned medium containing Wnt3a (hereafter called Wnt3a medium), expressed a markedly higher alkaline phosphatase (AP) activity than cells cultured in a control conditioned medium (hereafter called L medium) (Figure 1A). Real-time PCR revealed that *AP* mRNA levels steadily increased during the first 3 days of Wnt3a treatment before reaching a plateau (Figure 1C). Similarly, expression of *bone sialoprotein* (*Bsp*) was activated within the first 24 hr and reached a plateau by 72 hr of Wnt3a treatment (Figure 1C). On the other hand, *osteocalcin* (*OC*), a marker for mature osteoblasts, was induced only after 96 hr of Wnt3a stimulation (Figure 1C). Interestingly, Wnt3a did not stimulate *Runx2* expression, but it significantly induced *Osterix* (*Osx*) after 96 hr (Figure 1C). Moreover, in the presence of ascorbic acid and β-glycerophosphate, Wnt3a induced the widespread formation of mineralized nodules (Figure 1B). Finally, purified recombinant Wnt3a dose dependently induced AP in ST2 cells in a serum-free medium (Figure 1D). Thus, Wnt3a is sufficient to induce osteoblast differentiation in ST2 cells.

To identify downstream molecules responsible for Wnt-induced osteoblastogenesis, a proteomics approach was taken to compare protein profiles in ST2 cells cultured in Wnt3a medium versus L medium. Meristoylated alanine-rich C kinase substrate (MARCKS), a prototypic substrate for protein kinase C (PKC) (Blackshear, 1993), was detected at an increased level after 24 hr of Wnt3a stimulation (Figure 1E, arrows), a result confirmed by western analyses of total cell lysates (Figure 1F). As MARCKS is known to redistribute from the plasma membrane to the cytosol after phosphorylation (Arbuzova et al., 2002), the cytosolic fractions of cells were therefore analyzed for the levels of phosphorylated MARCKS by using a phospho-specific antibody. These studies revealed that MARCKS phosphorylation was markedly enhanced after 1 hr of incubation in Wnt3a medium, and that upregulation was sustained for at least 24 hr (Figure 1G). In fact, when cells were stimulated with purified Wnt3a without serum, phospho-MARCKS was readily detectable at 10 min post-stimulation, and levels steadily rose within the first hour (Figure 1H). Thus, Wnt3a robustly induces MARCKS phosphorylation in ST2 cells.

PKCδ Mediates Wnt3a-Induced Osteoblastogenesis, Independent of β-Catenin

Induction of MARCKS phosphorylation prompted us to examine the role of PKC in Wnt3a-induced osteoblastogenesis. The PKC family of serine and threonine protein kinases consists of at least 11 members, including the classic PKC isoforms (α, β1, β2, γ) activated by diacylglycerol (DAG), phosphatidylserine, and Ca^{2+}; the novel PKC subfamily (δ, ε, η, θ) activated by DAG and phosphatidylserine; and the atypical PKC isoforms (λ, ι, ζ) activated only by phosphatidylserine (Newton, 1997). Ro-31-8220, an inhibitor for all PKC isoforms, significantly impaired AP induction by Wnt3a (Figure 2A). However, Gö 6976, an inhibitor specific for classic PKC, had no effect even at 10 μM (IC_{50} 2.3 nM for PKCα, 6.7 nM for PKCβ) (Figure 2A). Similarly, the intracellular Ca^{2+} chelator BAPTA/AM did not inhibit Wnt3a-induced AP expression (Figure 2A). In addition, a peptide inhibitor specific for atypical PKC (PKCζ pseudosubstrate) also failed to inhibit Wnt3a-induced osteoblastogenesis (data not shown). In contrast, rottlerin, a selective inhibitor for PKCδ and PKCθ, significantly reduced AP induction in a dose-dependent manner (Figure 2A), but a PKCθ pseudosubstrate had no effect

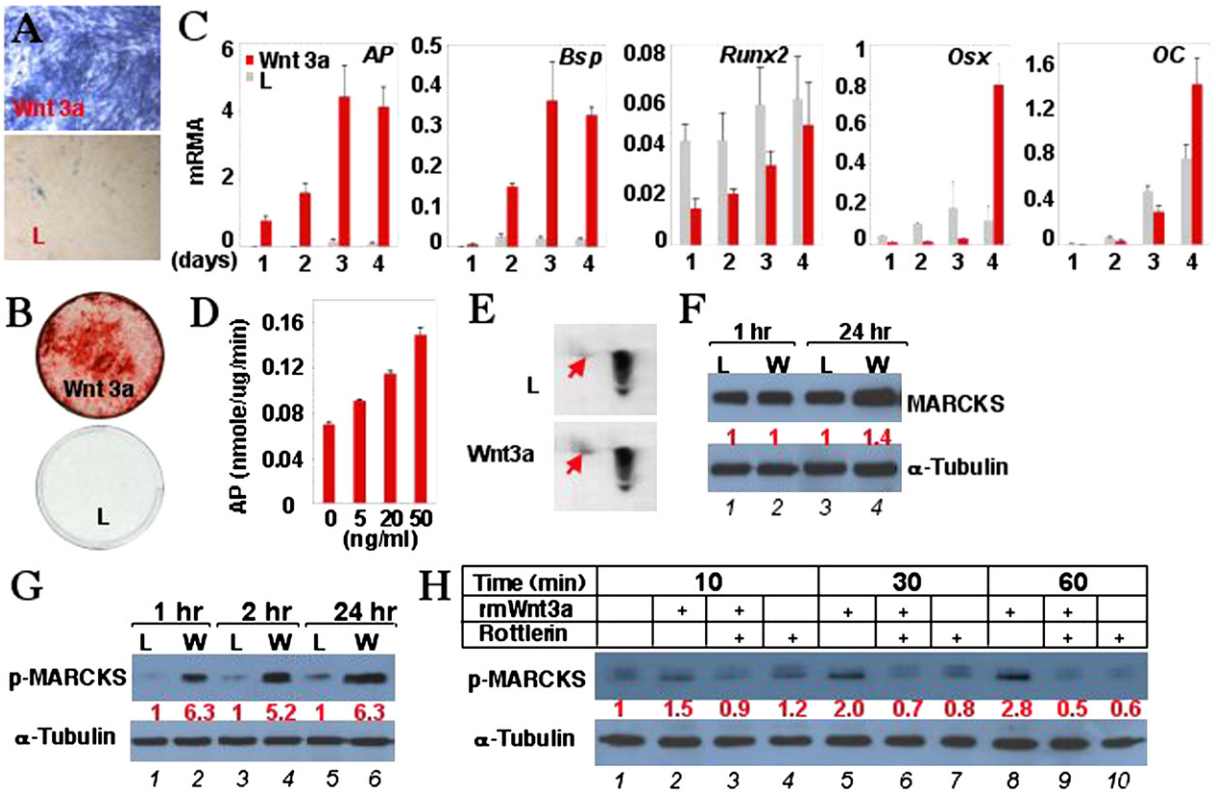

Figure 1. Wnt3a Induces Osteoblast Differentiation and MARCKS Phosphorylation via PKCδ in ST2 Cells

(A) AP detection by substrate staining after incubation for 48 hr in conditioned medium.

(B) Detection of bone nodules by alizarin red after incubation for 14 days in mineralization medium.

(C) Real-time PCR assays of mRNA expressed as folds over *GAPDH*.

(D) AP expression in cells cultured for 48 hr in serum-free medium with recombinant Wnt3a.

(E) Upregulation of MARCKS (arrows) by Wnt3a.

(F) Western analyses of total MARCKS in whole-cell lysates from cells incubated in Wnt3a (W) or L medium.

(G) Western analyses of phospho-MARCKS in cytosolic fractions of cells.

(H) Western analyses of phospho-MARCKS in cytosolic fractions of cells incubated in serum-free medium. Wnt3a was used at 50 ng/ml, and rottlerin was used at 5 μM.

Bar graphs: n = 3. Western signals are normalized to α-tubulin.

(data not shown). The inhibition of osteoblastogenesis by rottlerin was confirmed by real-time PCR of osteoblast markers (Figure S1; see the Supplemental Data available with this article online). Similarly, rottlerin inhibited Wnt3a-induced AP activity in primary cultures of limb primordial cells, isolated from E13.5 mouse embryos and containing osteoprogenitors but no mature osteoblasts (Figure 2B). Moreover, rottlerin abolished Wnt3a-induced MARCKS phosphorylation in ST2 cells (Figure 1H). Thus, PKCδ is required for Wnt3a-induced osteoblast differentiation and MARCKS phosphorylation.

To determine whether inhibition of PKC interfered with canonical Wnt signaling, we examined the potential effect of Ro-31-8220 or rottlerin on Wnt3a-induced transcriptional activation of a *Lef1-luciferase* reporter as well as β-catenin stabilization. Not only did Ro-31-8220 not impair Wnt3a-induced luciferase expression or β-catenin stabilization, it synergized with Wnt3a (Figures 2C and 2D). The fact that Ro-31-8220 also inhibits GSK3β, a known negative regulator of canonical Wnt signaling, may explain this observation. Similarly, rottlerin did not impair Wnt3a-induced β-catenin stabilization (Figure 2D). Thus, PKCδ mediates Wnt-induced osteoblastogenesis independent of canonical Wnt signaling.

To corroborate the role of PKCδ, we knocked down its expression with siRNA. Western analyses confirmed that PKCδ siRNA reduced the protein level of PKCδ by ~66% (Figure 3E). Importantly, the knockdown decreased Wnt3a-induced AP induction by ~50% (Figure 3A). Similarly, overexpression of a dominant-negative form of PKCδ (PKCδ-ΔC) by using a retroviral vector severely impaired Wnt3a-induced AP expression (data not shown). Moreover, when cultured in a mineralization medium, cells expressing PKCδ-ΔC formed significantly fewer bone nodules than control cells expressing GFP (Figures 3G and 3H). These results support the conclusion that PKCδ activity is required in Wnt3a-induced osteoblast differentiation.

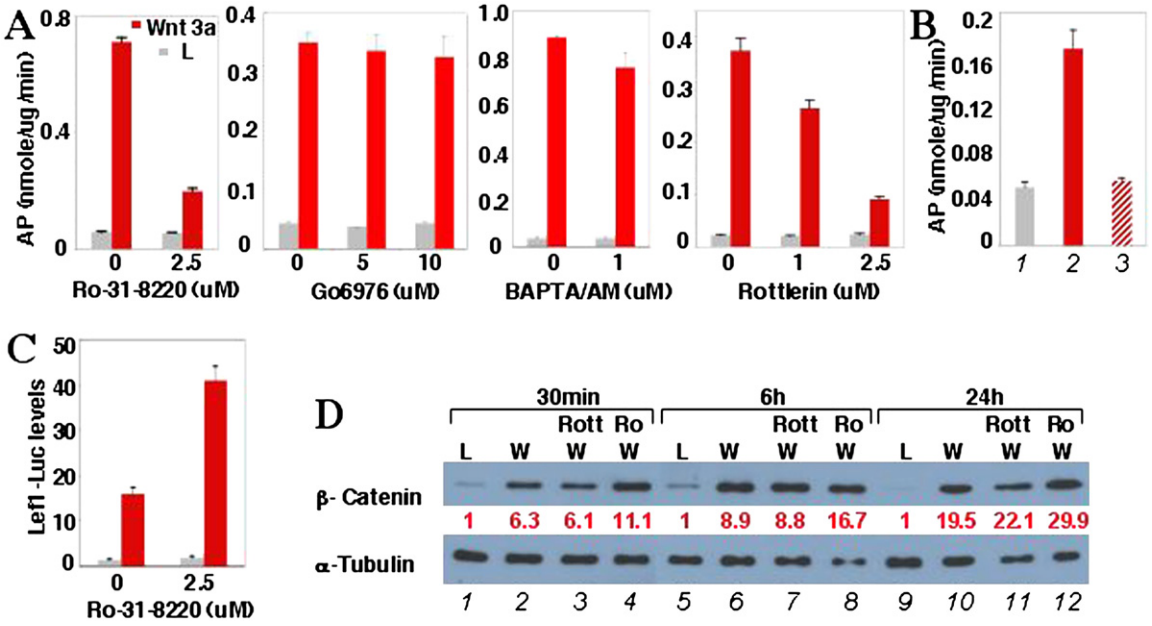

Figure 2. PKCδ Is Required for Wnt3a-Induced Osteoblastogenesis, but Not for Canonical Wnt Signaling in ST2 Cells

(A) Effects of PKC inhibitors on Wnt3a-induced AP expression in cells incubated for 48 hr in conditioned medium.

(B) Wnt3a-induced AP expression, and inhibition by rottlerin in primary E13.5 limb primordial cells after 96 hr of incubation. 1, L medium; 2, Wnt3a medium; 3, Wnt3a medium plus 5 μM rottlerin.

(C) Effect of Ro-31-8220 on Wnt3a-induced expression of *Lef1-luciferase* reporter.

(D) Western analyses of β-catenin in cytosolic fractions of cells after incubation in Wnt3a (W) or L medium, with or without 5 μM rottlerin (Rott) or Ro-31-8220 (Ro). When inhibitors were used, cells were pretreated with inhibitor for 1 hr in normal growth medium. Bar graphs: n = 3. The β-catenin level was normalized to α-tubulin.

G_q-Activated Phosphatidylinositol Signaling, Independent of β-Catenin, Mediates Wnt3a-Induced Osteoblastogenesis

We next set out to unravel the signaling cascade leading to PKCδ activation in response to Wnt3a. PKCδ is activated by DAG, which is, in turn, produced through hydrolysis of phosphatidylinositol 4,5-bisphosphate (PIP2) by phospholipase C (PLC). Since the PLC-β isoenzymes are activated by both the G_q subfamily of α subunits and the βγ subunits of heterotrimeric G proteins (Morris and Malbon, 1999), we examined whether G protein-linked phosphatidylinositol signaling was responsible for Wnt3a-induced PKCδ activation and subsequent osteoblastogenesis. Pertussis toxin, which catalyzes ADP ribosylation of the G_i family of the α subunits, thus uncoupling them from their activating receptors, is known to inhibit PLC-β activation by the βγ subunits (Morris and Malbon, 1999). The toxin, however, did not inhibit Wnt3a-induced osteoblast differentiation in ST2 cells (data not shown). We therefore focused subsequent studies on G_q signaling.

To examine the role of G_q signaling in Wnt-induced osteoblastogenesis, we took advantage of a dominant-negative reagent, G_qI, which is a COOH-terminal peptide (aa 305–359) of $G\alpha_q$ previously shown to partially inhibit G_q signaling (Akhter et al., 1998). G_qI expression significantly reduced Wnt3a-induced AP expression (Figure 3B), as well as bone nodule formation (Figures 3I and 3J). Thus, G_q signaling likely mediates Wnt3a-induced osteoblastogenesis.

To confirm the role of the G_q subfamily of α subunits, we reduced the levels of $G\alpha_q$ and $G\alpha_{11}$, two widely expressed members, with siRNA. A combination of siRNA oligonucleotides against $G\alpha_q$ or $G\alpha_{11}$ reduced their combined protein levels by ~43%, as detected by an antibody recognizing both molecules (Figure 3F). Importantly, these oligonucleotides reduced Wnt3a-induced AP expression by >50% (Figure 3C). Similarly, single knockdowns of either $G\alpha_q$ or $G\alpha_{11}$ also partially inhibited AP induction (data not shown). Thus, both $G\alpha_q$ and $G\alpha_{11}$ are likely to mediate Wnt3a-induced osteoblast differentiation.

To further test the function of phosphatidylinositol signaling, we examined the effect of U73122, a PLC inhibitor, on Wnt3a-induced osteoblastogenesis. U73122 not only inhibited AP induction by ~50% (Figure 3D), but it also reduced bone nodule formation (Figures 3K and 3L). Thus, PLC activity is important for Wnt-induced osteoblast differentiation.

Next, we examined whether inhibition of G_q signaling or PLC activity affected Wnt3a-induced PKCδ activation or β-catenin stabilization. Both U73122 (Figure 3M) and G_qI (Figure 3N) markedly reduced phospho-MARCKS, without significantly altering β-catenin stabilization. These results indicate that Wnt3a activates a $G\alpha_{q/11}$ → PLCβ → PKCδ pathway independent of β-catenin signaling to promote osteoblast differentiation.

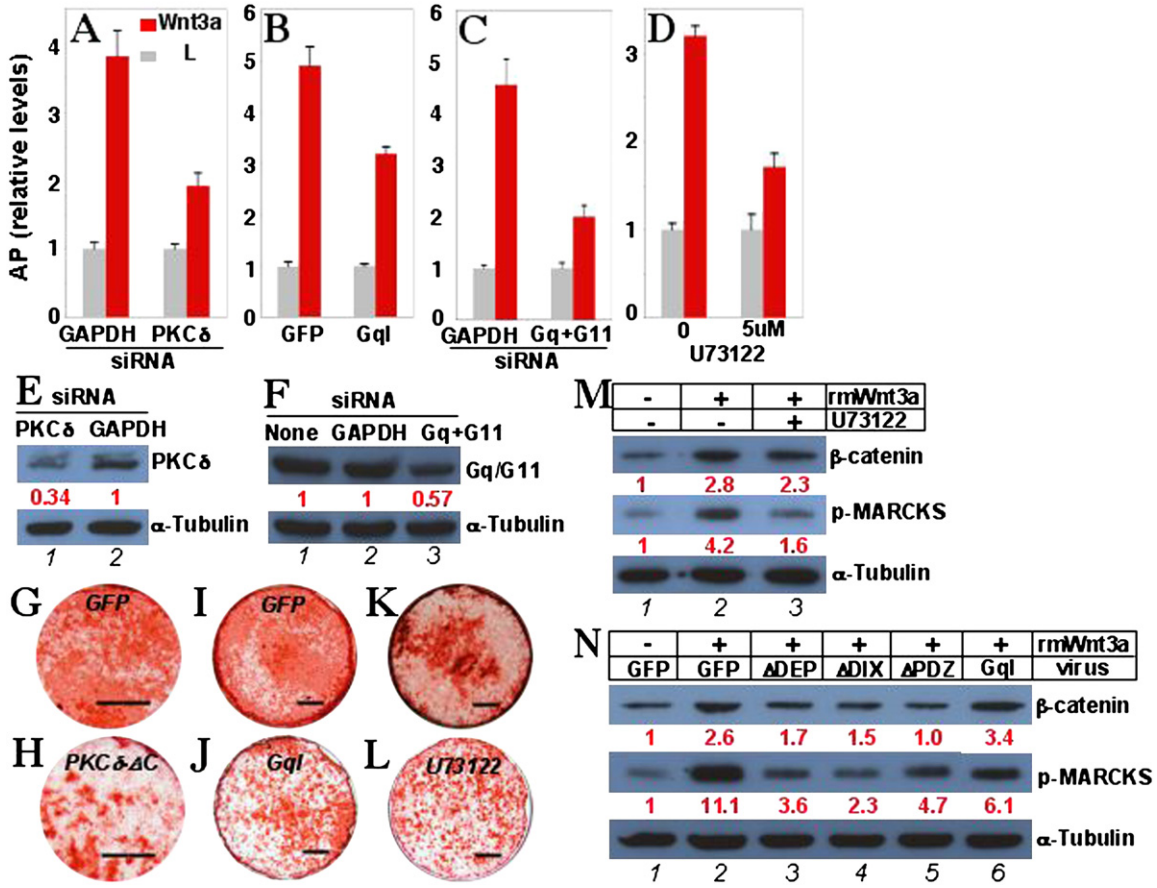

Figure 3. PKCδ Activation via G_q Signaling Promotes Wnt3a-Induced Osteoblastogenesis and Requires Dvl in ST2 Cells

(A–D) AP expression in cells incubated for 48 hr in conditioned medium. In (A) and (C), cells transfected with siRNA were incubated in normal growth medium for 96 hr before being cultured in conditioned medium. In (B), cells were first infected with retrovirus before being incubated in conditioned medium. n = 3.

(E and F) Western analyses for (E) PKCδ and (F) $G\alpha_q/G\alpha_{11}$ in whole-cell lysates of cells at 96 hr after siRNA transfection, with *GAPDH* siRNA as control.

(G–L) Detection of bone nodules by alizarin red. In (G)–(J), cells were infected with retrovirus before being incubated in Wnt3a-mineralization medium. U73122 was used at 5 μM.

(M and N) Western analyses for β-catenin and phospho-MARCKS in cytosolic fractions. Cells prestarved for 24 hr were cultured in serum-free medium for 1 hr with or without recombinant Wnt3a. In (N), cells were first infected with viruses, and then starved for 24 hr before Wnt3a stimulation. Western signals were normalized to α-tubulin.

PKCδ Activation by Wnt3a Requires Dvl, but Is Insensitive to Dkk1

We next examined whether PKCδ activation involves the Dvl family of molecules. Immunostaining revealed that in unstimulated ST2 cells, both PKCδ and Dvl-2 were present diffusely in the cytosol (Figures 4E–4G). However, within 30 min of Wnt3a stimulation, both molecules were translocated to the plasma membrane in a punctate pattern, although some signal remained in the perinuclear region (Figures 4A and 4B). Remarkably, PKCδ and Dvl-2 colocalized at the plasma membrane (Figure 4C). Similar results were observed with Dvl-1 and Dvl-3 (Figures S2 and S3). Thus, Wnt3a signaling translocates PKCδ and Dvl to common domains within the plasma membrane.

To determine the kinetics of membrane translocation for PKCδ and Dvl-2, we used western analyses to quantify the levels of these proteins in the cytosol after Wnt3a stimulation. At 10 min poststimulation, both PKCδ and Dvl-2 were markedly reduced in the cytosol (Figure 4I, lane 2). At 30 min, the cytosolic content of PKCδ or Dvl-2 was partially recovered but remained significantly lower than the prestimulation level (Figure 4I, lane 3). Interestingly, at 60 min, both proteins were present in the cytosol at a higher than prestimulation level (Figure 4I, lane 4). Consistent with activation of PKCδ at the cell membrane, the levels of phospho-MARCKS in the cytosol steadily rose within the first hour of stimulation (Figures 1H and 4I). Thus, concurrent with PKCδ activation, Wnt3a signaling acutely and transiently translocates PKCδ and Dvl-2 to the plasma membrane with similar kinetics.

We next examined whether Dvl signaling is required for PKCδ activation. Since the DIX, PDZ, and DEP domains

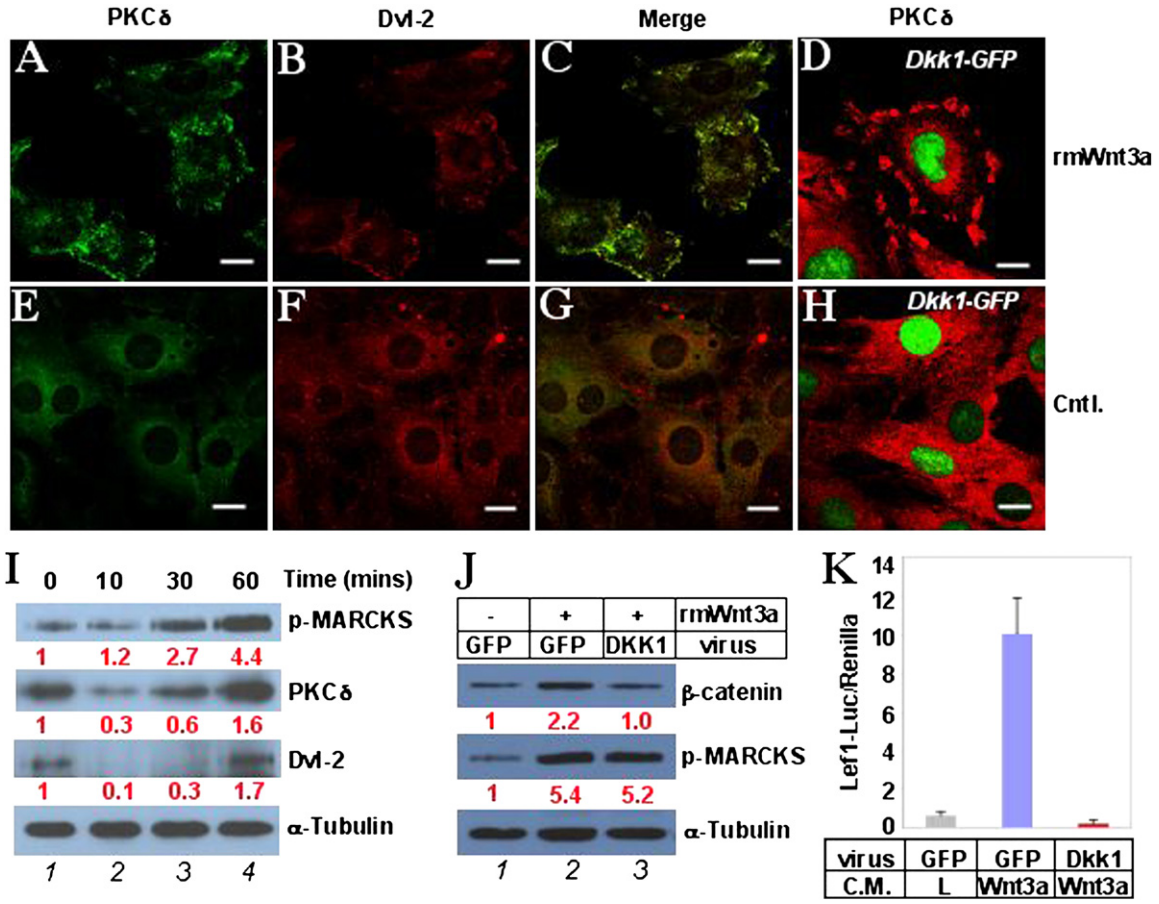

Figure 4. PKCδ Activation by Wnt3a Correlates with Dvl-2 Translocation to the Plasma Membrane and Is Insensitive to Dkk1 in ST2 Cells

(A–H) Immunostaining of PKCδ and Dvl-2 in cells (A–D) with or (E–H) without Wnt3a stimulation. In (D) and (H), cells were infected with a retrovirus coexpressing Dkk1 and nuclear GFP (*Dkk1-GFP*).

(I–J) Western analyses in cytosolic fractions. Cells were prestarved in serum-free medium for 24 hr before being stimulated with recombinant Wnt3a for (I) the indicated times or for (J) 1 hr. In (J), cells were first infected with retroviruses expressing either GFP or Dkk1 before starvation. Signal levels were normalized to α-tubulin.

(K) The effect of Dkk1 on *Lef1-luciferase* activation by Wnt3a. n = 3.

were reported to preferentially mediate distinct Wnt pathways, we set out to evaluate whether overexpression of Dvl-2 variants lacking one of the three conserved domains (ΔDIX, ΔPDZ, and ΔDEP) (Habas et al., 2001) differentially affects Wnt3a-induced PKCδ activation versus β-catenin stabilization. Cells expressing any of the Dvl-2 variants showed a marked reduction in MARCKS phosphorylation (Figure 3N). Similarly and unexpectedly, all three Dvl-2 variants also inhibited β-catenin accumulation (Figure 3N). These results support the conclusion that Dvl proteins are required for both PKCδ activation and β-catenin stabilization in response to Wnt3a, and that all three conserved domains may participate in both pathways.

To determine whether the Wnt-PKCδ pathway requires LRP5/6 signaling, we examined whether the membrane translocation of PKCδ in response to Wnt3a is sensitive to Dkk1 inhibition. Here, cells infected with a retrovirus coexpressing Dkk1 and nuclear GFP were immunostained for endogenous PKCδ, with or without Wnt3a stimulation. As in control cells (Figure 4A), Wnt3a induced characteristic translocation of PKCδ from the cytosol (Figure 4H) to the plasma membrane (Figure 4D) in cells overexpressing Dkk1. Thus, Dkk1 does not inhibit Wnt3a-induced membrane translocation of PKCδ.

We next examined whether Dkk1 inhibits Wnt3a-induced PKCδ activation. To this end, cytosolic proteins from virally infected cells with or without Wnt3a stimulation were assayed for phospho-MARCKS by western analyses. As a control for the efficacy of the Dkk1 virus, β-catenin levels were also analyzed. In addition, the virally infected cells were transfected with the *Lef1-luciferase* reporter and were assayed for response to Wnt3a. As expected, in Dkk1-overexpressing cells, Wnt3a failed to either stabilize β-catenin (Figure 4J) or activate transcription of the reporter (Figure 4K). On the other hand, Wnt3a induced phosphorylation of MARCKS in these cells

in a manner similar to that in the control cells (Figure 4J). Thus, in contrast to the canonical Wnt pathway, Wnt-PKCδ signaling does not appear to engage the LRP5/6 coreceptors.

Genetic Deletion of *PKCδ* Results in a Reduction in Embryonic Bone Formation

To determine the role of PKCδ in bone formation in vivo, we analyzed the skeleton of *PKCδ* knockout mice (*PKCδ*$^{-/-}$). The *PKCδ*$^{-/-}$ animals are viable and fertile but were reported to exhibit hyperactivation of B cell proliferation and auto-immunity (Miyamoto et al., 2002), as well as deficiency in stress-induced apoptosis of blood vessel smooth muscle cells (Leitges et al., 2001). We reasoned that removal of PKCδ might lead to quantitative defects more evident during early phases of bone formation, and we therefore focused our analyses on early embryos. At E15.5, the wild-type embryos showed obvious ossification in the maxilla, the mandible, the ribs, and the limbs (Figure 5A). In contrast, *PKCδ*$^{-/-}$ littermates exhibited much less ossification (Figure 5B). In particular, the maxilla and the mandible of mutant embryos showed only minimal mineralization compared with wild-type littermates (Figure 5, compare [C] and [D]). In limbs, bone collars of ossifying skeletal elements were notably shorter in the mutant embryo (Figure 5E). Accordingly, *von Kossa* staining on sections of long bones showed that bone collars were shortened in mutants at both E14.5 and E15.5 (Figure 5F). Indeed, the relative bone collar length normalized to the total skeletal element length was significantly reduced in the mutant (Figure 5G). Thus, removal of *PKCδ* results in less bone in the early embryonic skeleton.

As bone collar formation in the embryo is coupled with cartilage development, we examined the status of chondrocyte maturation in *PKCδ*$^{-/-}$ versus wild-type littermates. At E14.5, in mutant embryos, the hypertrophic zone expressing *Colα1(X)* was shortened; the domains expressing *parathyroid hormone-related peptide-receptor* (*PTHrP-R*) and *Indian hedgehog* (*Ihh*) were less well separated, and the terminal hypertrophic zone expressing *matrix metalloproteinase 13* (*MMP 13*) was reduced (Figure 5H). Thus, loss of PKCδ delays chondrocyte maturation in long bones.

We next examined whether progression of osteoblast differentiation was perturbed in *PKCδ*$^{-/-}$ embryos. To this end, we took advantage of the fact that osteoblastogenesis in the perichondrium of long bones progresses linearly along the epiphysis to diaphysis axis. In particular, the onset of expression for later osteoblast markers is coupled with chondrocyte maturation, resulting in characteristic positioning of the leading edge in relation to the hypertrophic cartilage. Thus, we examined the expression of a panel of osteoblast markers in the perichondrium by in situ hybridization, and we evaluated whether their positioning against the *Colα1(X)*-expressing hypertrophic chondrocytes on adjacent sections was altered in *PKCδ*$^{-/-}$ versus wild-type littermates at E15.5. In the wild-type embryo, the early markers *AP* (Figure 5I, arrow), *Colα1(I)*, and *Runx2* (data not shown) were detected throughout much of the metaphyseal perichondrium. On the other hand, *Osx* and *Bsp* were activated in perichondrial cells immediately preceding the hypertrophic region, with their leading edges (orange, vertical lines) positioned at a characteristic distance from the first row of *Colα1(X)*-positive cells (purple, vertical line) (Figure 5I). In the *PKCδ*$^{-/-}$ embryo, the expression patterns of *AP* (Figure 5I), *Colα1(I)*, and *Runx2* (data not shown) were similar to those in the wild-type littermates. However, the leading edges of *Osx* and *Bsp* (green, vertical lines) were significantly closer to the boundary of the hypertrophic zone (purple, vertical line) (Figure 5I). Thus, removal of *PKCδ* appears to delay the onset of *Osx* expression in the osteoblast lineage, which may, in turn, impede subsequent differentiation.

To confirm that loss of PKCδ results in intrinsic deficits in osteoblast differentiation, we performed in vitro osteoblastogenesis assays with primary cell cultures. We first assayed for bone nodule formation by E13.5 limb primordial cells. *PKCδ*$^{-/-}$ cells produced significantly fewer bone nodules than normal cells (Figure 5, compare [K] and [L]), but instead generated more cartilage nodules (Figure 5, compare [M] and [N]). Secondly, we assayed for AP production by primary bone marrow stromal cells (BMSCs) in culture. Here, *PKCδ*$^{-/-}$ BMSCs showed a significantly lower level than wild-type cells (Figure 5O). These results therefore support the conclusion that PKCδ in skeletal progenitor cells promotes osteoblast differentiation.

Lastly, we examined MARCKS phosphorylation levels in the cytosol of E14.5 limb primordial cells. The level of phospho-MARCKS was markedly lower in *PKCδ*$^{-/-}$ cells than in wild-type cells (Figure 5J). Thus, MARCKS is likely an endogenous substrate of PKCδ in vivo.

Wnt7b Induces Osteoblastogenesis via a Noncanonical, PKCδ-Dependent Mechanism

To assess the physiological relevance of Wnt-PKCδ signaling in bone formation, we investigated whether Wnt7b, a ligand expressed by osteogenic cells in vivo and able to induce osteoblast differentiation in vitro (Hu et al., 2005), signals through this pathway. In keeping with the previous finding, overexpression of Wnt7b, either by transient transfection (Figure 6F) or by viral infection (Figure 6G), induced AP expression in the multipotent mouse embryonic mesenchymal cell line C3H10T1/2 (Taylor and Jones, 1979). Moreover, Wnt7b overexpression induced formation of bone nodules in both C3H10T1/2 and ST2 cells in mineralization medium (Figure 6A). Finally, Wnt7b also induced osteoblast differentiation in primary cultures of E13.5 limb primordial cells (Figure 6H). Interestingly, in the limb cells, Wnt7b induced more robust osteoblastogenesis than a dominant active form of β-catenin (daβcat) (Figure 6H), even though >90% cells expressed daβcat, as judged by coexpression of GFP (data not shown). Thus, Wnt7b activates the osteogenic program in multiple cell systems, and activation may include alternative pathways to that mediated by β-catenin.

We next examined whether Wnt7b activates the canonical or the PKCδ pathway in the cell cultures. Wnt7b failed

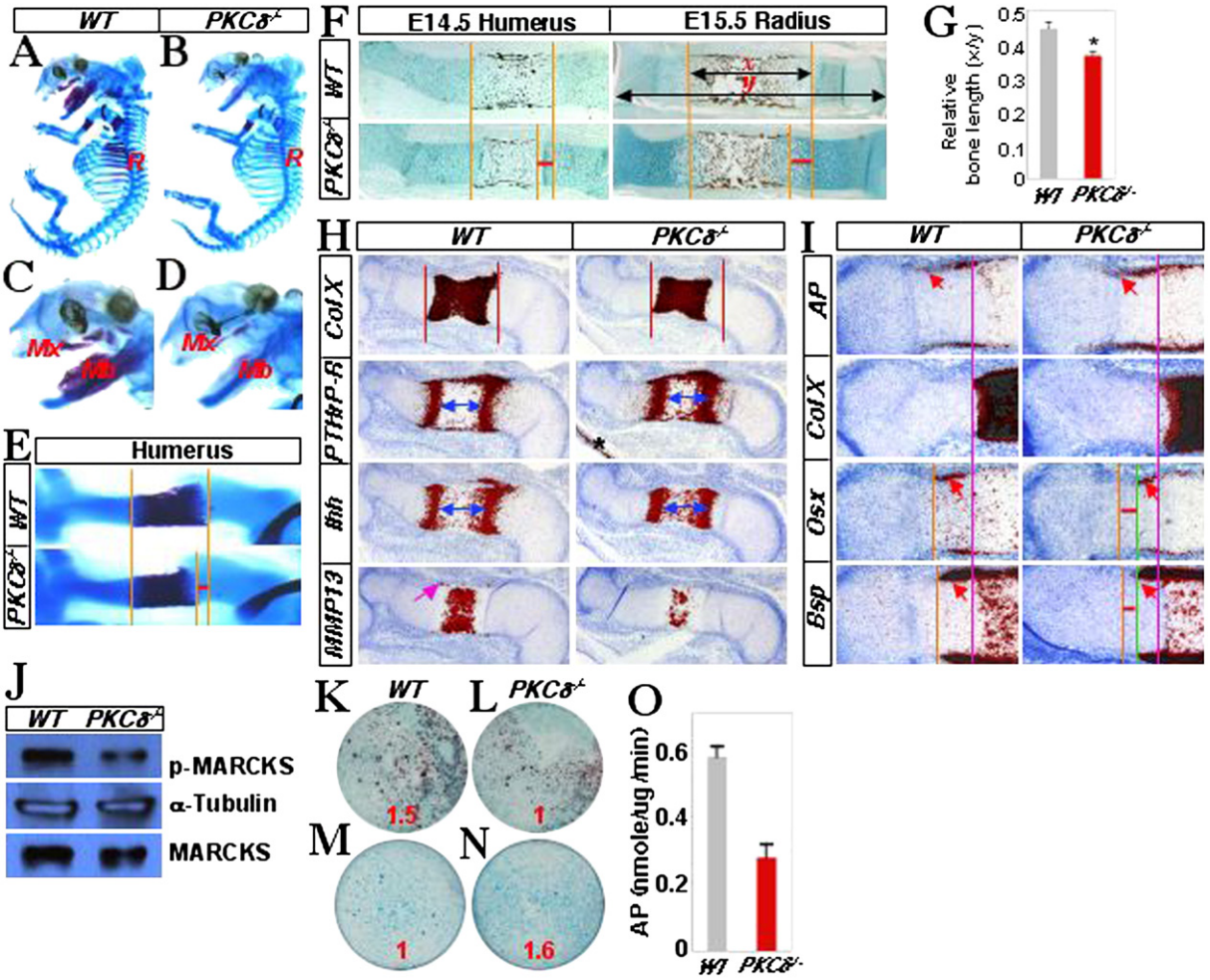

Figure 5. Removal of *PKCδ* Results in a Deficit in Embryonic Bone Formation

(A–E) Whole-mount skeletal staining of wild-type and *PKCδ*$^{-/-}$ littermates at E15.5. Bone stained red; cartilage stained blue. Vertical lines in (E) demarcate the ends of the bone collar; the horizontal, red line denotes the deficit in the mutant. R, ribs; Mx, maxilla; Mb, mandible.

(F) *von Kossa* staining on longitudinal sections of E14.5 humerus and E15.5 radius in wild-type versus *PKCδ*$^{-/-}$ littermates. Vertical lines demarcate the ends of the bone collar; the horizontal, red line denotes the deficit in the mutant. Double-headed arrows indicate the lengths of the bone collar (x) and the total radius (y).

(G) Relative bone length (x/y) in the radius of E15.5 wild-type versus *PKCδ*$^{-/-}$ embryos. n = 4, $p < 0.001$.

(H) In situ hybridization for chondrocyte markers on longitudinal sections of the humerus in wild-type versus *PKCδ*$^{-/-}$ E14.5 littermates. Vertical lines denote the ends of the *Colα1(X)*-expressing domain in the wild-type embryo. Double-headed arrows indicate the wild-type distance between two major *PTHrP-R* and *Ihh* expression domains. Asterisk, *PTHrP-R* signal in skin; arrow, *MMP13* signal in the osteoblast-lineage cell.

(I) In situ hybridization for osteoblast markers on longitudinal sections of tibia in wild-type versus *PKCδ*$^{-/-}$ littermates at E15.5. Adjacent sections are used for each genotype. Purple, vertical lines: leading edge of the *Colα1(X)*-expressing domain; orange, vertical lines: leading edge of *Osx* or *Bsp* in wild-type embryo; green, vertical lines: leading edge of *Osx* or *Bsp* in the *PKCδ*$^{-/-}$ embryo; red, horizontal lines: deficit in the *PKCδ*$^{-/-}$ embryo. Arrows, signal in perichondrium.

(J) Western analyses of cytosolic fractions of limb primordial cells from E14.5 wild-type versus *PKCδ*$^{-/-}$ littermates.

(K–N) Detection of (K and L) bone and (M and N) cartilage nodules in primary cultures of limb primordial cells from E13.5 (K and M) wild-type versus (L and N) *PKCδ*$^{-/-}$ embryos. Bone nodules stained dark red; cartilage nodules stained blue. Relative nodule numbers between normal and mutant genotypes were indicated.

(O) AP expression by wild-type versus *PKCδ*$^{-/-}$ BMSCs at 72 hr after confluence. n = 3.

to activate *Lef1-Luciferase* expression in either ST2 or C3H10T1/2 cells, even though Wnt3a and daßcat greatly stimulated expression (Figures 6B and 6C). Accordingly, Wnt7b failed to stabilize β-catenin in C3H10T1/2 cells (Figure 6E, top panel). On the other hand, Wnt7b induced MARCKS phosphorylation in both ST2 (Figure 6D) and C3H10T1/2 cells (Figure 6E). Thus, Wnt7b does not stimulate canonical Wnt signaling in either ST2 or C3H10T1/2 cells, but it activates PKCδ in both cell types.

We then evaluated the potential role of canonical versus PKCδ signaling in Wnt7b-induced osteoblastogenesis. Coexpression of Dkk1 did not impair AP induction by

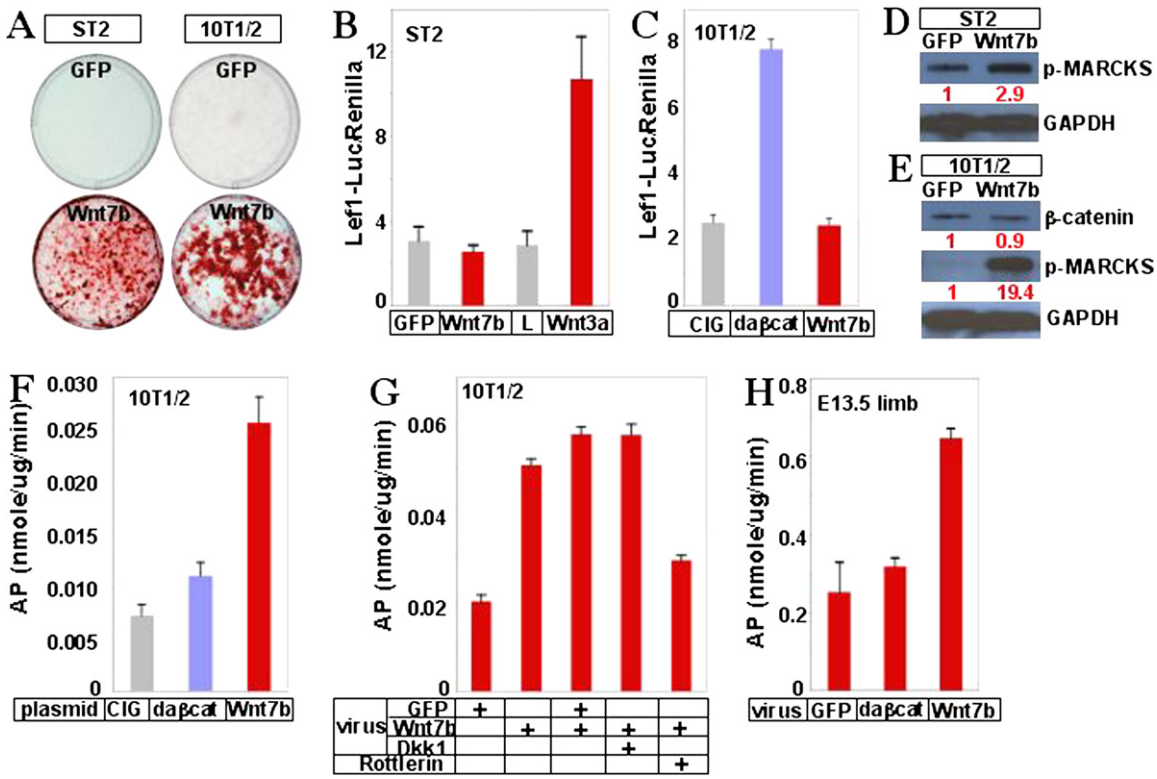

Figure 6. Wnt7b Induces Osteoblastogenesis and PKCδ Activity, but Does Not Activate Canonical Wnt Signaling

(A) Detection of bone nodules by alizarin red in ST2 and C3H10T1/2 cells expressing GFP or Wnt7b.

(B and C) *Lef1-luciferase* activation by Wnt3a, Wnt7b, or daßcat. In (B), Wnt7b was virally expressed, whereas Wnt3a was present in conditioned medium. In (C), cells were cotransfected with the reporter and a daßcat- or Wnt7b-expressing plasmid or with the empty expression vector pCIG. n = 3.

(D and E) Western analyses in cytosolic fractions of (D) ST2 or (E) C3H10T1/2 cells virally expressing GFP or Wnt7b, after incubation in serum-free medium for 24 hr. Western signals were normalized to GAPDH.

(F–H) AP expression in (F and G) C3H10T1/2 or (H) primary cultures of E13.5 limb primordial cells. Cells either (F) transiently transfected or (G and H) virally infected were cultured in normal growth medium for (F and G) 48 hr or (H) 72 hr. n = 3.

Wnt7b in either C3H10T1/2 (Figure 6G) or the primary limb primordial cells (data not shown). However, rottlerin strongly inhibited Wnt7b-induced AP activity in both cell types (Figure 6G and data not shown). Thus, Wnt7b induces osteoblast differentiation in multiple cell systems via the PKCδ-mediated noncanonical mechanism.

Genetic Ablation of *Wnt7b* Results in Deficiency in Embryonic Bone Formation

To assess the physiological role of Wnt7b in bone formation, we genetically removed *Wnt7b* from the skeletal progenitors by using the *Cre-loxP* technique. An initial report examining E18.5 embryos devoid of Wnt7b failed to show any clear skeletal phenotype (Rodda and McMahon, 2006). Here, we generated *Wnt7b* mutant mice (*Dermo1-Cre; Wnt7b$^{n/c3}$*) carrying a *Wnt7b* null allele (*Wnt7b^{n}*) (Parr et al., 2001), a *Wnt7b* conditional allele (*Wnt7b^{c3}*; J.R., T.J.C., and A.P.M., unpublished data), and also a *Dermo1-Cre* allele (Yu et al., 2003). The *Wnt7b^{c3}* allele had *loxP* sites flanking the essential exon 3 and functioned as a null allele upon recombination by Cre (to be reported elsewhere). *Wnt7b* mutant animals were viable after birth and had no obvious phenotype. However, whole-mount skeletal staining revealed that, at E15.5, when wild-type embryos showed obvious ossification, *Wnt7b* mutant littermates exhibited a diminution in ossification, while some mutant embryos also appeared to be slightly smaller (Figure 7A). Regardless of the overall size, the bone collar of long bones was consistently shorter in mutant littermates (Figure 7B), as confirmed by quantitation of the relative bone collar length over total length of the element (Figure 7C). At E18.5, mutant skulls exhibited less alizarin red staining and widened sutures (Figure 7D). Thus, Wnt7b deficiency results in less bone in mouse embryos.

We next examined whether chondrocyte maturation was perturbed in *Wnt7b* mutants. At E14.5, the overall length of the hypertrophic zone expressing *Colα1(X)* was similar between mutant and wild-type littermates (Figure 7F). However, in mutants, the domains expressing *PTHrP-R* or *Ihh* were less well separated, and the terminal hypertrophic region expressing *MMP13* was clearly reduced. At E15.5, the distance between the two *Colα1(X)*-expressing domains was significantly reduced in the

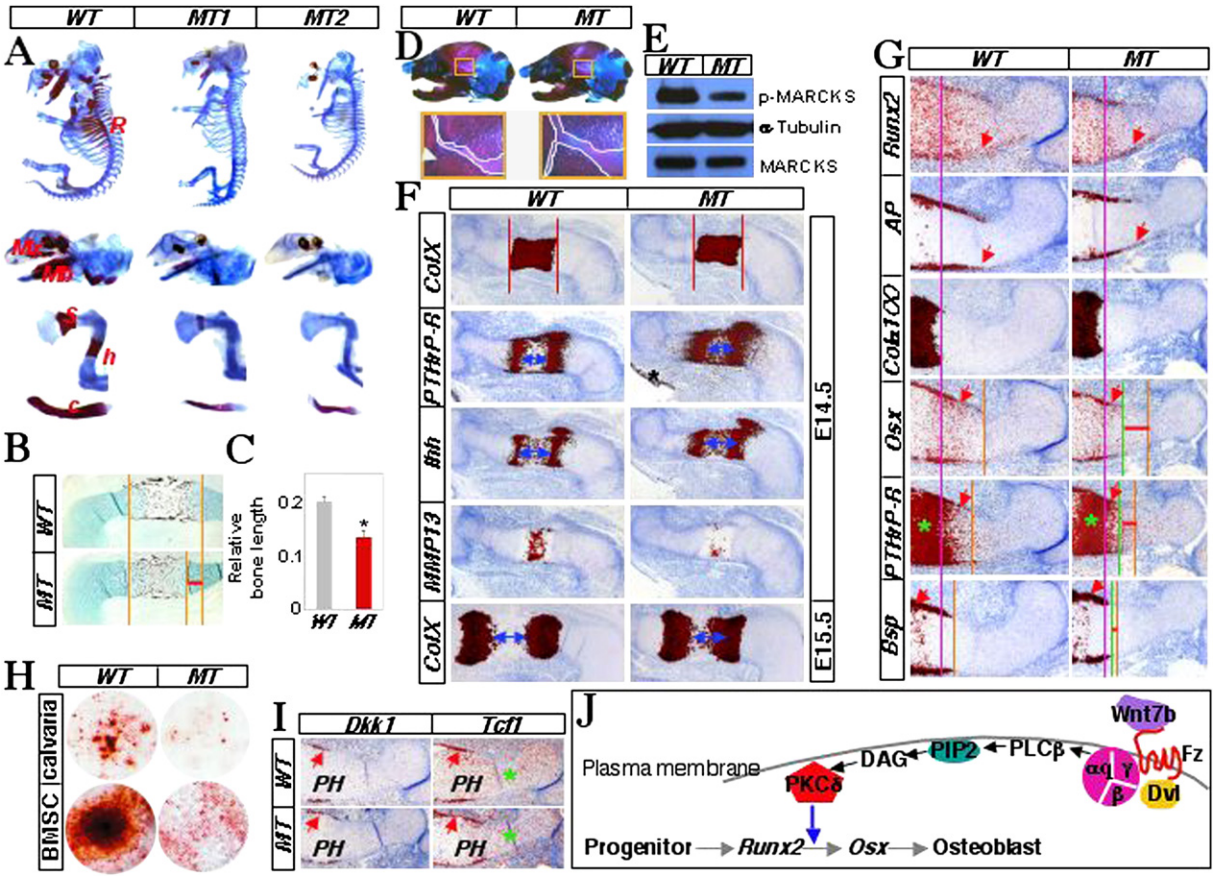

Figure 7. Removal of *Wnt7b* in Skeletal Cells Results in Defects in Bone Formation

(A) Whole-mount skeletal staining of wild-type (*WT*) or *Wnt7b* mutant (*MT1* and *MT2*) littermates at E15.5. Note the smaller size of *MT2*. Representative bones shown at a higher magnification below the corresponding whole skeleton. R, ribs; Mx, Maxilla; Mb, mandible; s, scapula; h, humerus; c, clavicle.

(B) *von Kossa* staining on longitudinal sections of humerus in wild-type (*WT*) versus *Wnt7b* mutant (*MT*) E15.5 littermates. Vertical lines demarcate the length of the bone collars; the horizontal line denotes the deficit in the mutant embryo.

(C) Relative bone length (bone collar over total length) in the humerus of wild-type versus *Wnt7b* mutant E14.5 littermates. n = 5; $p < 0.001$.

(D) Skulls of wild-type (*WT*) or *Wnt7b* mutant (*MT*) littermates at E18.5. Boxed regions are shown at a higher magnification below. The white contour demarcates sutures; the arrow denotes a nearly fused suture.

(E) Western analyses of cytosolic fractions of limb primordial cells from wild-type versus *Wnt7b* mutant E14.5 littermates.

(F) In situ hybridization for chondrocyte markers on longitudinal sections of the humerus from wild-type (*WT*) versus *Wnt7b* mutant (*MT*) embryos. Vertical lines denote the ends of the *Colα1(X)*-expressing domain in the wild-type embryo. Double-headed arrows indicate the wild-type distance between the two major *PTHrP-R*, *Ihh*, or *Colα1(X)* expression domains. Asterisk, *PTHrP-R* signal in skin.

(G) In situ hybridization for osteoblast markers on longitudinal sections of the humerus in wild-type versus *Wnt7b* mutant (*MT*) E15.5 littermates. Adjacent sections were used for each genotype. Purple, vertical lines: leading edge of the *Colα1(X)*-expressing domain in each genotype; orange, vertical lines: leading edge of *Osx*, *PTHrP-R*, or *Bsp* in wild-type; green, vertical lines: leading edge of *Osx*, *PTHrP-R*, or *Bsp* in the *MT* embryo; red, horizontal lines: deficit in the *MT* embryo. Arrows, signal in perichondrium; asterisks, signal in chondrocytes.

(H) Detection of bone nodules in primary cultures of calvarial cells or bone marrow stromal cells (BMSCs) from wild-type (*WT*) or *Wnt7b* mutant (*MT*) littermates.

(I) In situ hybridization for *Dkk1* and *Tcf1* on longitudinal sections of the humerus at E15.5. Asterisks, signal in chondrocytes; arrows, signal in perichondrium; *PH*, prehypertrophic chondrocytes.

(J) Wnt7b signals through a $G\alpha_{q/11} \rightarrow PLC\beta \rightarrow PKC\delta$ pathway to stimulate progression from *Runx2*- to *Osx*-expressing cells during osteoblastogenesis.

mutant. Thus, loss of Wnt7b appears to delay subsequent maturation of chondrocytes after the initiation of *Colα1(X)* expression.

To examine potential intrinsic defects in the osteoblast lineage, we assayed the expression of *AP*, *Bsp*, *Runx2*, *Osx*, and *PTHrP-R* in relation to *Colα1(X)* on adjacent sections of E15.5 long bones. Whereas *AP* and *Runx2* expression in the perichondrium was indistinguishable between mutant and wild-type littermates, the leading edges for *Osx*, *PTHrP-R*, and *Bsp* were consistently closer to the boundary of the hypertrophic zone in the mutant (Figure 7G). Thus, removal of *Wnt7b*, similar to that of

PKCδ, results in a deficit in *Osx* activation and subsequent osteoblast differentiation.

To determine whether removal of *Wnt7b* disrupted canonical Wnt signaling in long bones, we performed in situ hybridization for *Dkk1* and *Tcf1*, two known target genes of the pathway. Both molecules were expressed normally in *Wnt7b* mutant embryos (Figure 7I). In contrast, the limb primordial cells from E14.5 mutant embryos contained a significantly lower level of phospho-MARCKS than wild-type littermates (Figure 7E), indicating that Wnt7b stimulates MARCKS phosphorylation in vivo. Thus, the bone defect in *Wnt7b* mutant embryos is unlikely due to disruption of canonical Wnt signaling, but it appears to correlate with impairment in PKCδ activation.

To confirm that Wnt7b directly regulates osteoblast differentiation, we evaluated *Wnt7b*-deficient cells for their ability to differentiate in vitro. We utilized calvarial cells from neonates, as well as BMSCs from adult mice, both of which contain osteoblast precursors. In both cases, *Wnt7b*-deficient cells produced significantly fewer bone nodules than wild-type cells (Figure 7H). These results are consistent with the notion that endogenous Wnt7b promotes osteoblast differentiation from progenitors.

In summary, to our knowledge, the present study reveals a novel osteogenic pathway in which Wnt molecules, such as Wnt7b, signal through the G_q family of G protein α subunits to activate PKCδ, which, in turn, promotes the transition from *Runx2*- to *Osx*-expressing cells (Figure 7J).

DISCUSSION

We have delineated a noncanonical Wnt pathway that operates in mammalian osteoblast precursors to promote bone formation. In this pathway, Wnt activates the G protein-linked phosphatidylinositol signaling and subsequently PKCδ, via a mechanism that requires Dvl but is insensitive to Dkk1. Several lines of evidence support that Wnt7b, expressed in osteogenic tissues in vivo, stimulates osteoblast differentiation, likely through the PKCδ-mediated pathway. First, genetic ablation of either *Wnt7b* or *PKCδ* delayed the onset of *Osx* expression and reduced embryonic bone; second, *Wnt7b*- or *PKCδ*-deficient osteoprogenitors were defective in osteoblastogenesis in vitro; third, deletion of either gene reduced MARCKS phosphorylation in vivo.

G Proteins and Wnt Signaling

Although the $G\alpha_o$ subunit was recently found to mediate both the Wnt and the planar polarity pathway in *Drosophila* (Katanaev et al., 2005), the role of G proteins in Wnt signaling in mammals is not clear. In mouse F9 teratocarcinoma cells, overexpression of chimeric receptors between the β2-adrenergic receptor and rat Frizzled 1 or 2, was reported to activate the canonical Wnt pathway (Liu et al., 2001) or decrease intracellular cGMP (Ahumada et al., 2002), respectively, both in a pertussis toxin-sensitive manner. More recently, both $G\alpha_o$ and $G\alpha_q$ were found to mediate Wnt3a-induced stabilization of β-catenin in cell cultures (Liu et al., 2005). However, the physiological relevance of these findings is not known. Finally, adenylyl cyclase signaling was implicated in Wnt-induced myogenesis (Chen et al., 2005), but a direct role of G proteins remains to be confirmed.

The present study indicates that the G_q family of α subunits is required for Wnt-induced PKCδ activation, but not β-catenin stabilization in osteoprogenitors, and that G_q signaling is important for Wnt-induced osteoblast differentiation. These conclusions are supported by studies with a dominant-negative reagent (G_qI) and specific siRNA oligonucleotides against $G\alpha_q$ and $G\alpha_{11}$. Of note, mice missing both alleles of $G\alpha_q$ and one copy of $G\alpha_{11}$ ($G\alpha_q^{-/-}$; $G\alpha_{11}^{+/-}$) developed to term, but exhibited severe bone defects in the craniofacial skeleton (Offermanns et al., 1998). In addition, in *Xenopus* embryos, G_q, but not G_i, signaling mediated XWnt8a-induced axis duplication as well as mesoderm ventralization (Wu et al., 2000), although it was not clear whether in that system G_q signaled through β-catenin or an alternative pathway. Finally, it may be of interest to examine whether similar G protein signaling mediates cardiomyocyte differentiation induced by Wnt11, previously reported to be independent of β-catenin signaling (Koyanagi et al., 2005; Pandur et al., 2002).

Canonical versus Noncanonical Wnt Signaling

The mechanism for activating canonical versus noncanonical pathways by Wnt molecules is not clear. Wnt3a signaled through both the β-catenin and the PKCδ pathway in ST2 cells, whereas Wnt7b selectively activated the later in multiple cell types. The two pathways differed not only in their dependence on the LRP5/6 coreceptor, but also in their requirement for G_q signaling. This could indicate that Wnt3a induces the formation of two distinct signaling complexes or a single complex with dual signaling properties. The specificity of signaling complexes may be dictated by the Frizzled receptor(s), as forced expression of mouse Frizzled 4 in HEK293 cells (Mikels and Nusse, 2006) or human Frizzled 5 in *Xenopus* embryos (He et al., 1997) was sufficient to transduce canonical signaling by Wnt5a, which was otherwise inactive in this regard. Moreover, overexpression of different mouse Frizzled molecules in the *Xenopus* embryo was found to activate either classic PKC or downstream target genes of β-catenin (Sheldahl et al., 1999). Finally, Wnts may signal through receptors other than Frizzleds, such as the atypical receptor kinase Ryk (Lu et al., 2004; Schmitt et al., 2006) or the orphan receptor tyrosine kinase Ror2 (Mikels and Nusse, 2006). Identification of responsible Frizzled or alternative receptors for different Wnts under physiological conditions will help to elucidate the mechanism for Wnt ligands to generate distinct signals.

Wnt7b, PKCδ, and Bone Formation

Consistent with the role of Wnt-PKCδ signaling in osteoblastogenesis in vitro, genetic ablation of either *Wnt7b* or *PKCδ* resulted in a deficit in bone formation in the mouse embryo. Nonetheless bone formed in both mutants. The modest phenotype could reflect overlapping

roles of other Wnts or PKC isoforms important for osteoblastogenesis. Alternatively, Wnt-PKCδ signaling could represent a mechanism that augments other osteogenic signals, but itself is not essential for osteoblast differentiation in vivo. In this scenario, the noncanonical pathway appears to perform a function distinct from that of canonical Wnt signaling, as thus far inferred from genetic studies of β-catenin (Day et al., 2005; Hill et al., 2005; Hu et al., 2005; Rodda and McMahon, 2006).

The mechanism for Wnt7b and PKCδ to regulate the onset of *Osx* expression is presently unknown. Although an immediate target of Wnt-PKCδ signaling, MARCKS has not been implicated in bone formation. The *MARCKS*$^{-/-}$ mice had severe defects in neural development and exhibited perinatal lethality (Stumpo et al., 1995), but analyses of the skeletons of these mutant embryos have so far not revealed any obvious defects (data not shown). It is possible that other PKCδ substrates mediate osteoblast differentiation.

Frizzled-G Protein Signaling as a Target for Bone Anabolic Therapeutics

The present study identified a novel, to our knowledge, mechanism for Wnt signals to stimulate bone formation. Importantly, this pathway can be uncoupled from canonical Wnt signaling and is mediated through specific G proteins that are likely coupled with the Frizzled receptors. Thus, reagents that selectively activate G protein signaling by the relevant receptors may provide specific bone anabolic effects.

EXPERIMENTAL PROCEDURES

Plasmids and Oligonucleotides

Full-length *Wnt7b* cDNA was purchased from ATCC. The *Lef1-luciferase* reporter (Mao et al., 2001b) and the cDNAs for the dominant active form of β-catenin (Tetsu and McCormick, 1999), GqI (Akhter et al., 1998), and Dvl-2 derivatives (Habas et al., 2001) were as previously described. The full-length cDNA for *PKCδ* was cloned by PCR from a mouse E15 Marathon-Ready cDNA pool (BD Biosciences Clontech), and the cDNA for the truncated form (PKCδ-ΔC, aa 1–338) was generated by a second PCR from the full-length cDNA. The siRNA oligonucleotides for PKCδ were purchased from Dharmacon, and those for $G\alpha_q$ and $G\alpha_{11}$ were purchased from Ambion.

Antibodies, Proteins, and Chemicals

The polyclonal antibodies against PKCδ and MARCKS; the monoclonal antibodies against α-tubulin, Dvl-1, Dvl-2, and Dvl-3; and the HRP-conjugated secondary antibodies were purchased from Santa Cruz Biotechnology. The monoclonal antibodies against glyceraldehyde-3-phosphate dehydrogenase (GAPDH) and β-catenin were purchased from Chemicon and BD Biosciences Pharmigen, respectively. The polyclonal antibody against phospho-MARCKS was purchased from Cell Signaling. The polyclonal antibody against $G\alpha_q$ and $G\alpha_{11}$ was purchased from Calbiochem. The Alexa 488- or 555-conjugated secondary antibodies were purchased from Molecular Probes. Purified recombinant Wnt3a was purchased from R&D systems. All inhibitors for PKC and PLC were purchased from Calbiochem.

Cell Cultures

C3H10T1/2 cells, Wnt3a-expressing cells, and control L cells were obtained from ATCC and were maintained in BME with 10% bovine serum (Atlas) as per instructions. ST2 cells (Dr. Steve Teitelbaum, Washington University) were maintained in α-MEM (Sigma). Unless otherwise indicated, ST2 cells were seeded at 1.5 × 10^4 cells/cm^2 overnight before experiments. Wnt3a- and L-conditioned medium were used at 1:2 dilution in normal growth medium. The Ultraculture serum-free medium was purchased from Cambrex.

Primary cultures of limb primordial cells were dissociated from the stylopod and zeugopod region of the forelimb of E13.5 mouse embryos; primary cultures of the calvarial cells were isolated from 2-day-old newborn mice. Cells were seeded at 1 × 10^5 cells/cm^2 in α-MEM with 10% bovine serum and were used without passage.

Primary cultures of the bone marrow stromal cells (BMSCs) were isolated from the femur and the tibia of 5-week-old mice and were plated in α-MEM with 15% bovine serum; medium was changed at day 3 and day 6. Cells were passed once at days 7–8 and were reseeded at 1 × 10^5 cells/cm^2 for AP or mineralization assays.

Infections and Transfections

Viruses expressing GFP or Dkk1 were as previously described (Hu et al., 2005). Viruses expressing Wnt7b, PKCδ, PKCδ-ΔC, G_qI, or the Dvl-2 derivatives were generated in the same manner, and all coexpressed nuclear GFP via an internal ribosome entry site (IRES). A proper dilution of each virus stock in appropriate growth medium was chosen to achieve >90% infection as per GFP detection. For infections, cells were incubated at about 50% confluency in virus-containing medium for 24 hr.

Transient transfections were performed with Lipofectamine (Invitrogen) and, in some cases, after cells were infected with viruses. Luciferase and AP assays were performed at 48 hr after transfection.

Transfections of siRNA oligonucleotides were performed with siPORT Amine (Ambion). Four distinct siRNA duplexes each for $G\alpha_q$ and $G\alpha_{11}$ were individually tested; two in each case were found to be effective and were used in experiments reported here. For PKCδ, a pool of four siRNA duplexes was used.

Osteoblast Differentiation Assays

AP expression was detected as previously described (Katagiri et al., 1994). When inhibitors were used, cells were pretreated with the inhibitor in normal growth medium for 1 hr. For mineralization assays, confluent cells were incubated in the presence of 50 μg/ml ascorbic acid and 50 mM β-glycerophosphate for 14–21 days. Real-time PCR for osteoblast markers was performed as previously described (Hu et al., 2005).

Proteomics, Western Analyses, and Immunocytochemistry

For proteomics, ST2 cells were cultured in Wnt3a or L medium for 24 hr before total cell lysates were harvested by using a lysis buffer containing a protease inhibitor cocktail (Roche) and phosphatase inhibitor cocktail 1 and 2 (Sigma). Proteomic analyses were performed at the Siteman Cancer Center Proteomics Core Facility (Washington University).

Western analyses were performed by using the ECL Plus Western Blotting Detection System (Amersham Biosciences). The intensity of protein bands was quantified with ImageJ (http://rsb.info.nih.gov/ij/). For analyses of mutant embryos, E14.5 limbs were skinned, homogenized, and extracted for cytosolic proteins in the presence of protease and phosphatase inhibitors.

Immunocytochemistry was performed on chamber slides (Nalge Nunc International). Cells seeded at 0.75 × 10^4/cm^2 were cultured overnight in regular medium, and then either directly switched to serum-free medium for 24 hr or first infected with retroviruses before changing to serum-free medium. Cells were then stimulated in fresh serum-free medium for 30 min with recombinant Wnt3a protein at 50 ng/ml, and cells were finally immunostained and examined by confocal microscopy.

Mouse Strains and Analyses

The *PKCδ*$^{+/-}$ (Miyamoto et al., 2002), the *Dermo1-Cre* (Yu et al., 2003), and the *Wnt7b*$^{+/-}$ (Parr et al., 2001) mouse strains were previously

described. Whole-mount skeletal staining, mouse embryo tissue processing, *von Kossa* staining, and in situ hybridization were performed as described (Hilton et al., 2005). To quantitate relative bone length, multiple sections representing different sectioning planes were stained by *von Kossa*, and ratios of bone collar length over total length of the element were calculated.

Supplemental Data

Supplemental Data include real-time PCR results showing the effects of rottlerin on cells treated with Wnt3a and immunostaining results showing Wnt3a-induced colocalization of PKCδ with Dvl-1 and Dvl-3 and are available at http://www.developmentalcell.com/cgi/content/full/12/1/113/DC1/.

ACKNOWLEDGMENTS

We are indebted to Drs. Xi He, Walter Koch, Christopher Niehrs, Frank McCormick, and Steve Teitelbaum for providing reagents. We thank Drs. Deborah Stumpo and Perry Blackshear (NIEHS) for sharing *MARCKS*$^{-/-}$ mouse embryos. The work was supported in part by National Institutes of Health grants R01 DK065789 (F.L.) and P01 DK056246 (A.P.M.). K.S.J. was supported by the Korea Science and Engineering Foundation.

Received: July 17, 2006
Revised: October 12, 2006
Accepted: November 3, 2006
Published: January 8, 2007

REFERENCES

Ahumada, A., Slusarski, D.C., Liu, X., Moon, R.T., Malbon, C.C., and Wang, H.Y. (2002). Signaling of rat Frizzled-2 through phosphodiesterase and cyclic GMP. Science *298*, 2006–2010.

Akhter, S.A., Luttrell, L.M., Rockman, H.A., Iaccarino, G., Lefkowitz, R.J., and Koch, W.J. (1998). Targeting the receptor-Gq interface to inhibit in vivo pressure overload myocardial hypertrophy. Science *280*, 574–577.

Arbuzova, A., Schmitz, A.A., and Vergeres, G. (2002). Cross-talk unfolded: MARCKS proteins. Biochem. J. *362*, 1–12.

Bafico, A., Liu, G., Yaniv, A., Gazit, A., and Aaronson, S.A. (2001). Novel mechanism of Wnt signalling inhibition mediated by Dickkopf-1 interaction with LRP6/Arrow. Nat. Cell Biol. *3*, 683–686.

Bennett, C.N., Longo, K.A., Wright, W.S., Suva, L.J., Lane, T.F., Hankenson, K.D., and MacDougald, O.A. (2005). Regulation of osteoblastogenesis and bone mass by Wnt10b. Proc. Natl. Acad. Sci. USA *102*, 3324–3329.

Blackshear, P.J. (1993). The MARCKS family of cellular protein kinase C substrates. J. Biol. Chem. *268*, 1501–1504.

Bodine, P.V., Zhao, W., Kharode, Y.P., Bex, F.J., Lambert, A.J., Goad, M.B., Gaur, T., Stein, G.S., Lian, J.B., and Komm, B.S. (2004). The Wnt antagonist secreted frizzled-related protein-1 is a negative regulator of trabecular bone formation in adult mice. Mol. Endocrinol. *18*, 1222–1237.

Boyden, L.M., Mao, J., Belsky, J., Mitzner, L., Farhi, A., Mitnick, M.A., Wu, D., Insogna, K., and Lifton, R.P. (2002). High bone density due to a mutation in LDL-receptor-related protein 5. N. Engl. J. Med. *346*, 1513–1521.

Cadigan, K.M., and Nusse, R. (1997). Wnt signaling: a common theme in animal development. Genes Dev. *11*, 3286–3305.

Chamorro, M.N., Schwartz, D.R., Vonica, A., Brivanlou, A.H., Cho, K.R., and Varmus, H.E. (2005). FGF-20 and DKK1 are transcriptional targets of β-catenin and FGF-20 is implicated in cancer and development. EMBO J. *24*, 73–84.

Chen, A.E., Ginty, D.D., and Fan, C.M. (2005). Protein kinase A signalling via CREB controls myogenesis induced by Wnt proteins. Nature *433*, 317–322.

Choi, S.C., and Han, J.K. (2002). *Xenopus* Cdc42 regulates convergent extension movements during gastrulation through Wnt/Ca^{2+} signaling pathway. Dev. Biol. *244*, 342–357.

Curtin, J.A., Quint, E., Tsipouri, V., Arkell, R.M., Cattanach, B., Copp, A.J., Henderson, D.J., Spurr, N., Stanier, P., Fisher, E.M., et al. (2003). Mutation of Celsr1 disrupts planar polarity of inner ear hair cells and causes severe neural tube defects in the mouse. Curr. Biol. *13*, 1129–1133.

Day, T.F., Guo, X., Garrett-Beal, L., and Yang, Y. (2005). Wnt/β-catenin signaling in mesenchymal progenitors controls osteoblast and chondrocyte differentiation during vertebrate skeletogenesis. Dev. Cell *8*, 739–750.

Glass, D.A., 2nd, Bialek, P., Ahn, J.D., Starbuck, M., Patel, M.S., Clevers, H., Taketo, M.M., Long, F., McMahon, A.P., Lang, R.A., and Karsenty, G. (2005). Canonical Wnt signaling in differentiated osteoblasts controls osteoclast differentiation. Dev. Cell *8*, 751–764.

Glinka, A., Wu, W., Delius, H., Monaghan, A.P., Blumenstock, C., and Niehrs, C. (1998). Dickkopf-1 is a member of a new family of secreted proteins and functions in head induction. Nature *391*, 357–362.

Gong, Y., Slee, R.B., Fukai, N., Rawadi, G., Roman-Roman, S., Reginato, A.M., Wang, H., Cundy, T., Glorieux, F.H., Lev, D., et al. (2001). LDL receptor-related protein 5 (LRP5) affects bone accrual and eye development. Cell *107*, 513–523.

Habas, R., Kato, Y., and He, X. (2001). Wnt/Frizzled activation of Rho regulates vertebrate gastrulation and requires a novel Formin homology protein Daam1. Cell *107*, 843–854.

Habas, R., Dawid, I.B., and He, X. (2003). Coactivation of Rac and Rho by Wnt/Frizzled signaling is required for vertebrate gastrulation. Genes Dev. *17*, 295–309.

He, X., Saint-Jeannet, J.P., Wang, Y., Nathans, J., Dawid, I., and Varmus, H. (1997). A member of the Frizzled protein family mediating axis induction by Wnt-5A. Science *275*, 1652–1654.

Heisenberg, C.P., Tada, M., Rauch, G.J., Saude, L., Concha, M.L., Geisler, R., Stemple, D.L., Smith, J.C., and Wilson, S.W. (2000). Silberblick/Wnt11 mediates convergent extension movements during zebrafish gastrulation. Nature *405*, 76–81.

Hill, T.P., Spater, D., Taketo, M.M., Birchmeier, W., and Hartmann, C. (2005). Canonical Wnt/β-catenin signaling prevents osteoblasts from differentiating into chondrocytes. Dev. Cell *8*, 727–738.

Hilton, M.J., Tu, X., Cook, J., Hu, H., and Long, F. (2005). Ihh controls cartilage development by antagonizing Gli3, but requires additional effectors to regulate osteoblast and vascular development. Development *132*, 4339–4351.

Hu, H., Hilton, M.J., Tu, X., Yu, K., Ornitz, D.M., and Long, F. (2005). Sequential roles of Hedgehog and Wnt signaling in osteoblast development. Development *132*, 49–60.

Huelsken, J., and Birchmeier, W. (2001). New aspects of Wnt signaling pathways in higher vertebrates. Curr. Opin. Genet. Dev. *11*, 547–553.

Katagiri, T., Yamaguchi, A., Komaki, M., Abe, E., Takahashi, N., Ikeda, T., Rosen, V., Wozney, J.M., Fujisawa-Sehara, A., and Suda, T. (1994). Bone morphogenetic protein-2 converts the differentiation pathway of C2C12 myoblasts into the osteoblast lineage. J. Cell Biol. *127*, 1755–1766.

Katanaev, V.L., Ponzielli, R., Semeriva, M., and Tomlinson, A. (2005). Trimeric G protein-dependent frizzled signaling in *Drosophila*. Cell *120*, 111–122.

Kato, M., Patel, M.S., Levasseur, R., Lobov, I., Chang, B.H., Glass, D.A., 2nd, Hartmann, C., Li, L., Hwang, T.H., Brayton, C.F., et al. (2002). Cbfa1-independent decrease in osteoblast proliferation, osteopenia, and persistent embryonic eye vascularization in mice deficient in Lrp5, a Wnt coreceptor. J. Cell Biol. *157*, 303–314.

Kibar, Z., Vogan, K.J., Groulx, N., Justice, M.J., Underhill, D.A., and Gros, P. (2001). Ltap, a mammalian homolog of *Drosophila* Strabismus/Van Gogh, is altered in the mouse neural tube mutant Loop-tail. Nat. Genet. *28*, 251–255.

Kinoshita, N., Iioka, H., Miyakoshi, A., and Ueno, N. (2003). PKC δ is essential for Dishevelled function in a noncanonical Wnt pathway that regulates *Xenopus* convergent extension movements. Genes Dev. *17*, 1663–1676.

Koyanagi, M., Haendeler, J., Badorff, C., Brandes, R.P., Hoffmann, J., Pandur, P., Zeiher, A.M., Kuhl, M., and Dimmeler, S. (2005). Non-canonical Wnt signaling enhances differentiation of human circulating progenitor cells to cardiomyogenic cells. J. Biol. Chem. *280*, 16838–16842.

Kuhl, M., Sheldahl, L.C., Malbon, C.C., and Moon, R.T. (2000). Ca(2+)/calmodulin-dependent protein kinase II is stimulated by Wnt and Frizzled homologs and promotes ventral cell fates in *Xenopus*. J. Biol. Chem. *275*, 12701–12711.

Lee, P.N., Pang, K., Matus, D.Q., and Martindale, M.Q. (2006). A WNT of things to come: evolution of Wnt signaling and polarity in cnidarians. Semin. Cell Dev. Biol. *17*, 157–167.

Leitges, M., Mayr, M., Braun, U., Mayr, U., Li, C., Pfister, G., Ghaffari-Tabrizi, N., Baier, G., Hu, Y., and Xu, Q. (2001). Exacerbated vein graft arteriosclerosis in protein kinase Cδ-null mice. J. Clin. Invest. *108*, 1505–1512.

Little, R.D., Carulli, J.P., Del Mastro, R.G., Dupuis, J., Osborne, M., Folz, C., Manning, S.P., Swain, P.M., Zhao, S.C., Eustace, B., et al. (2002). A mutation in the LDL receptor-related protein 5 gene results in the autosomal dominant high-bone-mass trait. Am. J. Hum. Genet. *70*, 11–19.

Liu, T., DeCostanzo, A.J., Liu, X., Wang, H., Hallagan, S., Moon, R.T., and Malbon, C.C. (2001). G protein signaling from activated rat frizzled-1 to the β-catenin-Lef-Tcf pathway. Science *292*, 1718–1722.

Liu, X., Rubin, J.S., and Kimmel, A.R. (2005). Rapid, Wnt-induced changes in GSK3β associations that regulate β-catenin stabilization are mediated by Gα proteins. Curr. Biol. *15*, 1989–1997.

Lu, W., Yamamoto, V., Ortega, B., and Baltimore, D. (2004). Mammalian Ryk is a Wnt coreceptor required for stimulation of neurite outgrowth. Cell *119*, 97–108.

Mao, B., Wu, W., Li, Y., Hoppe, D., Stannek, P., Glinka, A., and Niehrs, C. (2001a). LDL-receptor-related protein 6 is a receptor for Dickkopf proteins. Nature *411*, 321–325.

Mao, J., Wang, J., Liu, B., Pan, W., Farr, G.H., 3rd, Flynn, C., Yuan, H., Takada, S., Kimelman, D., Li, L., and Wu, D. (2001b). Low-density lipoprotein receptor-related protein-5 binds to Axin and regulates the canonical Wnt signaling pathway. Mol. Cell *7*, 801–809.

Mikels, A.J., and Nusse, R. (2006). Purified Wnt5a protein activates or inhibits β-catenin-TCF signaling depending on receptor context. PLoS Biol. *4*, e115.

Miyamoto, A., Nakayama, K., Imaki, H., Hirose, S., Jiang, Y., Abe, M., Tsukiyama, T., Nagahama, H., Ohno, S., Hatakeyama, S., and Nakayama, K.I. (2002). Increased proliferation of B cells and auto-immunity in mice lacking protein kinase Cδ. Nature *416*, 865–869.

Montcouquiol, M., Rachel, R.A., Lanford, P.J., Copeland, N.G., Jenkins, N.A., and Kelley, M.W. (2003). Identification of Vangl2 and Scrb1 as planar polarity genes in mammals. Nature *423*, 173–177.

Morris, A.J., and Malbon, C.C. (1999). Physiological regulation of G protein-linked signaling. Physiol. Rev. *79*, 1373–1430.

Newton, A.C. (1997). Regulation of protein kinase C. Curr. Opin. Cell Biol. *9*, 161–167.

Niida, A., Hiroko, T., Kasai, M., Furukawa, Y., Nakamura, Y., Suzuki, Y., Sugano, S., and Akiyama, T. (2004). DKK1, a negative regulator of Wnt signaling, is a target of the β-catenin/TCF pathway. Oncogene *23*, 8520–8526.

Offermanns, S., Zhao, L.P., Gohla, A., Sarosi, I., Simon, M.I., and Wilkie, T.M. (1998). Embryonic cardiomyocyte hypoplasia and craniofacial defects in G α q/G α 11-mutant mice. EMBO J. *17*, 4304–4312.

Ogawa, M., Nishikawa, S., Ikuta, K., Yamamura, F., Naito, M., and Takahashi, K. (1988). B cell ontogeny in murine embryo studied by a culture system with the monolayer of a stromal cell clone, ST2: B cell progenitor develops first in the embryonal body rather than in the yolk sac. EMBO J. *7*, 1337–1343.

Pandur, P., Lasche, M., Eisenberg, L.M., and Kuhl, M. (2002). Wnt-11 activation of a non-canonical Wnt signalling pathway is required for cardiogenesis. Nature *418*, 636–641.

Parr, B.A., Cornish, V.A., Cybulsky, M.I., and McMahon, A.P. (2001). Wnt7b regulates placental development in mice. Dev. Biol. *237*, 324–332.

Penzo-Mendez, A., Umbhauer, M., Djiane, A., Boucaut, J.C., and Riou, J.F. (2003). Activation of Gβγ signaling downstream of Wnt-11/Xfz7 regulates Cdc42 activity during *Xenopus* gastrulation. Dev. Biol. *257*, 302–314.

Pinson, K.I., Brennan, J., Monkley, S., Avery, B.J., and Skarnes, W.C. (2000). An LDL-receptor-related protein mediates Wnt signalling in mice. Nature *407*, 535–538.

Rodda, S.J., and McMahon, A.P. (2006). Distinct roles for Hedgehog and canonical Wnt signaling in specification, differentiation and maintenance of osteoblast progenitors. Development *133*, 3231–3244.

Schmitt, A.M., Shi, J., Wolf, A.M., Lu, C.C., King, L.A., and Zou, Y. (2006). Wnt-Ryk signalling mediates medial-lateral retinotectal topographic mapping. Nature *439*, 31–37.

Semenov, M.V., Tamai, K., Brott, B.K., Kuhl, M., Sokol, S., and He, X. (2001). Head inducer Dickkopf-1 is a ligand for Wnt coreceptor LRP6. Curr. Biol. *11*, 951–961.

Sheldahl, L.C., Park, M., Malbon, C.C., and Moon, R.T. (1999). Protein kinase C is differentially stimulated by Wnt and Frizzled homologs in a G-protein-dependent manner. Curr. Biol. *9*, 695–698.

Sheldahl, L.C., Slusarski, D.C., Pandur, P., Miller, J.R., Kuhl, M., and Moon, R.T. (2003). Dishevelled activates Ca^{2+} flux, PKC, and CamKII in vertebrate embryos. J. Cell Biol. *161*, 769–777.

Slusarski, D.C., Corces, V.G., and Moon, R.T. (1997). Interaction of Wnt and a Frizzled homologue triggers G-protein-linked phosphatidylinositol signalling. Nature *390*, 410–413.

Stumpo, D.J., Bock, C.B., Tuttle, J.S., and Blackshear, P.J. (1995). MARCKS deficiency in mice leads to abnormal brain development and perinatal death. Proc. Natl. Acad. Sci. USA *92*, 944–948.

Tada, M., and Smith, J.C. (2000). Xwnt11 is a target of *Xenopus* Brachyury: regulation of gastrulation movements via Dishevelled, but not through the canonical Wnt pathway. Development *127*, 2227–2238.

Tamai, K., Semenov, M., Kato, Y., Spokony, R., Liu, C., Katsuyama, Y., Hess, F., Saint-Jeannet, J.P., and He, X. (2000). LDL-receptor-related proteins in Wnt signal transduction. Nature *407*, 530–535.

Taylor, S.M., and Jones, P.A. (1979). Multiple new phenotypes induced in 10T1/2 and 3T3 cells treated with 5-azacytidine. Cell *17*, 771–779.

Tetsu, O., and McCormick, F. (1999). β-catenin regulates expression of cyclin D1 in colon carcinoma cells. Nature *398*, 422–426.

Veeman, M.T., Axelrod, J.D., and Moon, R.T. (2003). A second canon. Functions and mechanisms of β-catenin-independent Wnt signaling. Dev. Cell *5*, 367–377.

Wallingford, J.B., Rowning, B.A., Vogeli, K.M., Rothbacher, U., Fraser, S.E., and Harland, R.M. (2000). Dishevelled controls cell polarity during *Xenopus* gastrulation. Nature *405*, 81–85.

Wang, J., Mark, S., Zhang, X., Qian, D., Yoo, S.J., Radde-Gallwitz, K., Zhang, Y., Lin, X., Collazo, A., Wynshaw-Boris, A., and Chen, P. (2005). Regulation of polarized extension and planar cell polarity in the cochlea by the vertebrate PCP pathway. Nat. Genet. *37*, 980–985.

Wang, J., Hamblet, N.S., Mark, S., Dickinson, M.E., Brinkman, B.C., Segil, N., Fraser, S.E., Chen, P., Wallingford, J.B., and Wynshaw-Boris, A. (2006). Dishevelled genes mediate a conserved mammalian PCP pathway to regulate convergent extension during neurulation. Development *133*, 1767–1778.

Wodarz, A., and Nusse, R. (1998). Mechanisms of Wnt signaling in development. Annu. Rev. Cell Dev. Biol. *14*, 59–88.

Wu, C., Zeng, Q., Blumer, K.J., and Muslin, A.J. (2000). RGS proteins inhibit Xwnt-8 signaling in *Xenopus* embryonic development. Development *127*, 2773–2784.

Yu, K., Xu, J., Liu, Z., Sosic, D., Shao, J., Olson, E.N., Towler, D.A., and Ornitz, D.M. (2003). Conditional inactivation of FGF receptor 2 reveals an essential role for FGF signaling in the regulation of osteoblast function and bone growth. Development *130*, 3063–3074.